



Feathered Non-Avian Dinosaurs from North America Provide Insight into Wing Origins

Darla K. Zelenitsky *et al.*

Science **338**, 510 (2012);

DOI: 10.1126/science.1225376

This copy is for your personal, non-commercial use only.

If you wish to distribute this article to others, you can order high-quality copies for your colleagues, clients, or customers by [clicking here](#).

Permission to republish or repurpose articles or portions of articles can be obtained by following the guidelines [here](#).

The following resources related to this article are available online at www.sciencemag.org (this information is current as of March 10, 2013):

Updated information and services, including high-resolution figures, can be found in the online version of this article at:

<http://www.sciencemag.org/content/338/6106/510.full.html>

Supporting Online Material can be found at:

<http://www.sciencemag.org/content/suppl/2012/10/25/338.6106.510.DC1.html>

This article **cites 49 articles**, 13 of which can be accessed free:

<http://www.sciencemag.org/content/338/6106/510.full.html#ref-list-1>

This article appears in the following **subject collections**:

Paleontology

<http://www.sciencemag.org/cgi/collection/paleo>

the signal-to-noise ratio at close to micromolar concentrations (fig. S6). Alternatively, very fast kinetics—for example, in protein folding—could be resolved if the signal was large enough (29). Increasing the excitation power to only 7 μW (10 kW/cm^2) yielded fluorescence signals of up to 10.6 MHz, allowing the direct visualization of 10- μs blinking events (see fig. S7).

Self-assembled nanoantennas with docking sites based on DNA origami scaffolds represent an inexpensive and versatile platform to study plasmonic effects of metallic NP systems. The approach offers a simple solution to one of the urgent needs, that is, the ability to couple optical sources to nanoantennas. We have studied the dependence of the fluorescence intensity and lifetime of single dyes placed in the vicinity of gold NP monomers and dimers of varying sizes. We achieved fluorescence enhancement of up to 117-fold for 100-nm dimers that enables higher count rates in single-molecule applications and relaxes the requirements for single-molecule-compatible fluorescent dyes. Our results are in good agreement with numerical simulations and show that substantial fluorescence enhancement can be achieved, even at an interparticle distance of 23 nm that allows for the accommodation of biomolecular assays. The reduction of the hot-spot size far beyond diffraction-limited dimensions and the improved signal-to-noise ratio

pave the way for sensor applications and nano-scale light control and extend the concentration range of single-molecule measurements toward the biologically relevant micromolar regime.

References and Notes

1. C. Joo, H. Balci, Y. Ishitsuka, C. Buranachai, T. Ha, *Annu. Rev. Biochem.* **77**, 51 (2008).
2. P. Tinnefeld, M. Sauer, *Angew. Chem. Int. Ed.* **44**, 2642 (2005).
3. J. Eid *et al.*, *Science* **323**, 133 (2009).
4. B. Huang, H. Babcock, X. Zhuang, *Cell* **143**, 1047 (2010).
5. M. J. Levene *et al.*, *Science* **299**, 682 (2003).
6. S. Uemura *et al.*, *Nature* **464**, 1012 (2010).
7. L. Novotny, N. van Hulst, *Nat. Photonics* **5**, 83 (2011).
8. J. A. Schuller *et al.*, *Nat. Mater.* **9**, 193 (2010).
9. T. H. Taminiau, F. D. Stefani, F. B. Segerink, N. F. van Hulst, *Nat. Photonics* **2**, 234 (2008).
10. A. G. Curto *et al.*, *Science* **329**, 930 (2010).
11. A. Kinkhabwala *et al.*, *Nat. Photonics* **3**, 654 (2009).
12. M. Ringer *et al.*, *Phys. Rev. Lett.* **100**, 203002 (2008) and references therein.
13. H. Lin *et al.*, *ChemPhysChem* **13**, 973 (2012) and references therein.
14. H. Gang *et al.*, *Nature* **469**, 385 (2011) and references therein.
15. M. P. Busson, B. Rolly, B. Stout, N. Bonod, S. Bidault, *Nat. Commun.* **3**, 962 (2012) and references therein.
16. P. W. Rothmund, *Nature* **440**, 297 (2006).
17. S. M. Douglas *et al.*, *Nature* **459**, 414 (2009).
18. See the supplementary materials on Science Online.
19. G. P. Acuna *et al.*, *ACS Nano* **6**, 3189 (2012).
20. E. A. Coronado, E. R. Encina, F. D. Stefani, *Nanoscale* **3**, 4042 (2011).
21. P. Anger, P. Bharadwaj, L. Novotny, *Phys. Rev. Lett.* **96**, 113002 (2006).
22. A. Bek *et al.*, *Nano Lett.* **8**, 485 (2008).
23. S. Kühn, U. Håkanson, L. Rogobete, V. Sandoghdar, *Phys. Rev. Lett.* **97**, 017402 (2006).
24. J. Vogelsang *et al.*, *Angew. Chem. Int. Ed.* **47**, 5465 (2008).
25. N. Di Fiori, A. Meller, *Biophys. J.* **98**, 2265 (2010).
26. R. Jungmann *et al.*, *Nano Lett.* **10**, 4756 (2010).
27. S. A. McKinney, A.-C. Déclais, D. M. J. Lilley, T. Ha, *Nat. Struct. Biol.* **10**, 93 (2003).
28. A. Gietl, P. Holzmeister, D. Grohmann, P. Tinnefeld, *Nucleic Acids Res.* **40**, e110 (2012).
29. H. S. Chung, K. McHale, J. M. Louis, W. A. Eaton, *Science* **335**, 981 (2012).

Acknowledgments: We thank A. Gietl, J. J. Schmied, D. Grohmann, T. Liedl, and F. Stefani for fruitful discussion; A. Tiefnig for sample preparation; F. Demming for assistance with the numerical simulations; and S. Carregal Romero for the transmission electron microscopy images. This work was carried out at the NanoBioScience group, Braunschweig University of Technology, and was supported by a starting grant (SiMBA) of the European Research Council, the Volkswagen Foundation, and the Center for NanoScience. Technische Universität Braunschweig, G.P.A., and P.T. have filed a provisional patent application, EP1260316.1, on the described method of creating hotspots using self-assembled DNA origami.

Supplementary Materials

www.sciencemag.org/cgi/content/full/338/6106/506/DC1
Materials and Methods
Figs. S1 to S9
Table S1
References (30–34)

9 August 2012; accepted 25 September 2012
10.1126/science.1228638

Feathered Non-Avian Dinosaurs from North America Provide Insight into Wing Origins

Darla K. Zelenitsky,^{1*} François Therrien,^{2*} Gregory M. Erickson,³ Christopher L. DeBuhr,¹ Yoshitsugu Kobayashi,⁴ David A. Eberth,² Frank Hadfield⁵

Previously described feathered dinosaurs reveal a fascinating record of feather evolution, although substantial phylogenetic gaps remain. Here we report the occurrence of feathers in ornithomimosaurs, a clade of non-maniraptoran theropods for which fossilized feathers were previously unknown. The *Ornithomimus* specimens, recovered from Upper Cretaceous deposits of Alberta, Canada, provide new insights into dinosaur plumage and the origin of the avian wing. Individuals from different growth stages reveal the presence of a filamentous feather covering throughout life and winglike structures on the forelimbs of adults. The appearance of winglike structures in older animals indicates that they may have evolved in association with reproductive behaviors. These specimens show that primordial wings originated earlier than previously thought, among non-maniraptoran theropods.

Non-avian dinosaurs have been found in a variety of sediments worldwide, but skeletons with well-preserved feathers have been restricted to fine-grained deposits, primarily the Upper Jurassic and Lower Cretaceous lacustrine deposits of Liaoning, China (1–8). Although feathered dinosaur specimens have helped substantiate the dinosaurian origin of birds (2, 3, 9–12), their restricted occurrence has left notable gaps in the record of early feather

evolution, particularly among non-maniraptoran theropods (such as Ornithomimosauria or Carnosauria). Here we report on the presence of feathers in ornithomimosaurs (bird-mimic dinosaurs), based on specimens found in Upper Cretaceous fluvial channel deposits of Alberta, Canada, a discovery that expands the known phylogenetic, depositional, and geographic range of feathered non-avian dinosaurs. Three skeletons, referable to juvenile and adult *Ornithomimus*

edmontonicus (8), and housed at the Royal Tyrrell Museum of Palaeontology (TMP), collectively preserve evidence of filamentous and shafted feathers in this taxon. This occurrence of feathered non-avian dinosaurs in North America reveals the nature of ornithomimosaur plumage, provides insight into the origin of wings in Theropoda, and demonstrates new potential for the discovery of well-preserved feathered dinosaur specimens in fluvial (coarser-grained) deposits.

Two of the *Ornithomimus* specimens preserve filamentous feathers [type 1 or 2 feathers (11, 12)]. The first is the partial skeleton (TMP 2009.110.1) of a young juvenile (~1 year old) (8), which has filaments covering the axial and appendicular skeleton (Fig. 1). These integumentary structures, morphologically similar to the primitive filamentous feathers described in the Liaoning theropods (1, 2), are preserved as a dense array of hundreds of filaments in a thin (up to 2 mm) ferruginous coating that follows

¹Department of Geoscience, University of Calgary, Calgary, Alberta T2N 1N4, Canada. ²Royal Tyrrell Museum of Palaeontology, Drumheller, Alberta T0J 0Y0, Canada. ³Department of Biological Science, Florida State University, Tallahassee, FL 32306–4295, USA. ⁴Hokkaido University Museum, Hokkaido University, Sapporo, Hokkaido 060 0810, Japan. ⁵Palcoprep, Drumheller, Alberta T0J 0Y0, Canada.

*To whom correspondence should be addressed. E-mail: dkzeleni@ucalgary.ca (D.K.Z.); francois.therrien@gov.ab.ca (F.T.)

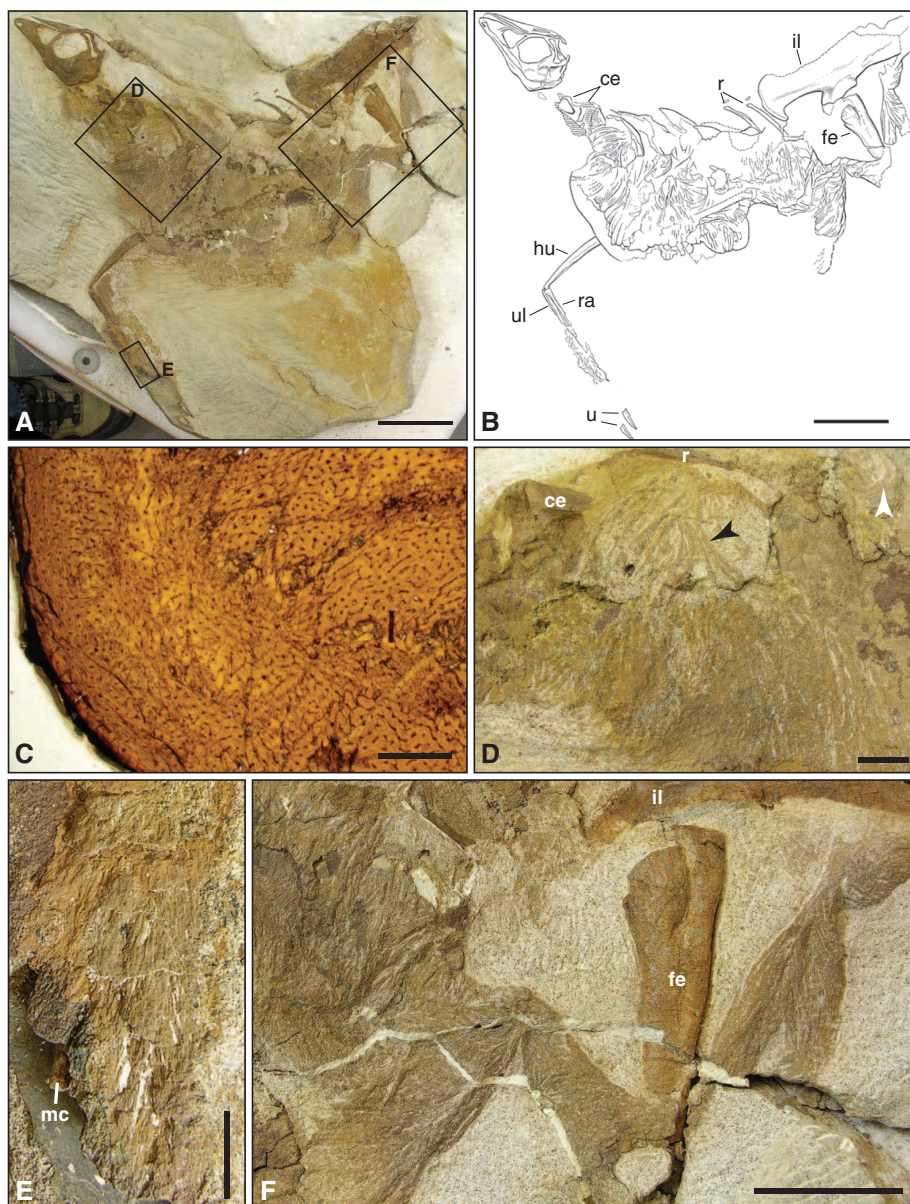
the three-dimensional (3D) contour of the body (Fig. 1, D to F). These structures (up to 50 mm in length and 0.5 mm in width) drape ventrally over the left side, perpendicular to the vertebral column, and run parallel or subparallel to one another. They are curved or contorted on some areas of the body, indicating that the original structures were supple (Fig. 1, D and F, and figs. S1 and S2). On the distal forelimbs, the filaments are shorter (up to 15 mm) than those on the body, and part at a low angle along the midline (Fig. 1E and fig. S3). Many of the filaments on the right manus show a central calcite streak (Fig. 1E and fig. S4), which indicates that the structures had a hollow core, as proposed for primitive filamentous feathers (1, 8, 11, 13, 14). The preservation of feathers within a ferruginous residue in a sandstone represents a previously undescribed preservational mode for non-avian feathers; however, other dinosaur soft tissues

have been found associated with such residues (15–17).

A second specimen (TMP 2008.70.1) is an incomplete adult skeleton lacking forelimbs (8), which displays filamentous feathers preserved as faint 2D carbonized traces along the neck, back, and anterior thorax (Fig. 2). The filaments, morphologically similar to those of TMP 2009.110.1 and the Liaoning theropods (1, 2), measure up to 50 mm long and 0.5 mm wide (8). They are in close contact with the bone on the ventral side of the skeleton and start approximately 20 mm from the bone on the dorsal side. Their orientation varies from subparallel to 50° relative to the bone surfaces, and their curvature indicates that the original structures were supple (Fig. 2B). Feather preservation resembles that of the Liaoning theropods (1, 2), although the filaments in TMP 2008.70.1 are faint, sparsely distributed, and preserved in a sandstone matrix.

Evidence of shafted feathers [i.e., feathers with a rigid shaft, with or without interlocking barbules [type 3 feathers or higher (11, 12)]] is preserved on the forelimb bones of an adult *Ornithomimus* skeleton (TMP 1995.110.1, Fig. 3). This specimen has an array of approximately 70 2D carbonized traces [a common preservational style for feathers (8, 18, 19)] as linear markings on the surfaces of the ulna and radius (Fig. 3, B and C). The markings on the ulna are located on the dorsal and posterior sides and change orientation gradually along its length, from posterodistally near the proximal end to longitudinally toward the distal end, whereas those on the radius are located on the dorsal side and are all oriented anterodistally. Their distribution and orientation are similar to the insertion pattern of covert feathers (20, 21), which form the bulk of the feather covering in modern bird wings. The shapes of the individual markings are consistent with

Fig. 1. Juvenile *Ornithomimus* (TMP 2009.110.1) preserving filamentous feather traces in ferruginous residue. (A) Photograph and (B) illustration of specimen showing the distribution and orientation of filamentous feathers and the location of insets. Scale bar, 10 cm. (C) Histological photomicrograph of metatarsal, showing highly vascularized bone lacking growth lines, indicating an individual less than 1 year old. Scale bar, 0.5 mm. (D) Close-up of filaments draping ventrally over the neck region, with curved filaments (white arrow) and possible filament bundles (black arrow). Scale bar, 2 cm. (E) Close-up of distal right forelimb, displaying filaments fanning out from the midline. Calcite infilled some feathers. Scale bar, 1 cm. (F) Close-up of feather filaments following the contour of abdomen and thigh. Scale bar, 5 cm. Interpretive line drawings of (D) to (F) are available in (8). ce, cervical vertebrae; fe, femur; hu, humerus; il, ilium; mc, metacarpal; ra, radius; r, rib; ul, ulna; u, ungual phalange.



the morphology of the rigid shafts of such feathers. The markings are up to 6.5 mm long and up to 1.5 mm wide (8) and are much wider than the filamentous feathers (0.5 mm) in the other two specimens. Almost all are linear features with well-defined (nondiffuse) edges, indicating that the original structures were elongate and straight. Some markings have an open central area and/or have U- or hook-shaped components (Fig. 3C). Such 2D shapes are consistent with traces that would be left by longitudinal or oblique sections of an originally elongate and hollow structure, such as a feather calamus (8). Based on the distribution, orientation, anatomical location, size, and shape of these markings on the bones, we interpret them as traces of the calami of covert feathers that covered the forearm in *Ornithomimus*.

The *Ornithomimus* specimens reveal two distinct plumages during ontogeny (Fig. 4, A and B). Young juveniles (~1 year old) had a plumage of filamentous feathers, whereas adults possessed both filamentous feathers and a pennibrachium [a winglike structure consisting of elongate feathers (22)]. This evidence for an ontogenetic change in plumage shows that immature individuals did not possess all the feather types present in adults. This indicates that the absence of specific feather types (such as remiges) in other feathered non-avian theropod taxa, especially those primarily known from immature individuals, could be partially due to their early ontogenetic stage, thus potentially complicating reconstruction of the evolutionary history of feathers and early wings.

The presence of a pennibrachium in ornithomimosaurs, previously reported only among maniraptorans (22), indicates that winglike structures originated earlier than previously known (Fig. 4C). Several roles have been proposed for primitive wings [gliding (23, 24), predatory behaviors (25, 26), or terrestrial locomotion (27, 28)], but their occurrence in a clade of ground-dwelling herbivorous (29) non-maniraptorans suggests that they did not originate for predatory behaviors or aerial locomotion. The *Ornithomimus* specimens show a late appearance of shafted wing feathers during ontogeny (occurring in adults but absent in 1-year-old juveniles) as compared to birds, in which these feathers develop early, within a few weeks of hatching (28, 30, 31), to be used for aerial (31) or terrestrial (28) locomotion. Although ornithomimosaurs may have also used their feathered forelimbs for terrestrial locomotion as in some birds (chukar and ostrich) (27, 28, 32, 33), the ontogenetically late appearance of the pennibrachia suggests that they may have initially evolved as a secondary sexual characteristic. As such, these winglike structures would have been used for reproductive activities (such as courtship, display, and brooding) and were only later, among maniraptorans, co-opted for other roles, including flight.

Until now, non-avian dinosaurs with well-preserved feathers had been recovered exclusively from fine-grained deposits, primarily in northeastern China (1–8). The present report of feathered ornithomimosaurs found in channel

sandstones from North America reveals that specimens bearing well-preserved feather impressions also occur in fluvial (coarser-grained) deposits. Such deposits have historically yielded a great abundance of dinosaur skeletons (34), yet associated feathers have heretofore gone unnoticed, perhaps because they are generally expected to be preserved only in finer-grained sediments (18, 19). The discovery of feathered dinosaurs in sandstone indicates that their integ-

umentary structures may be more readily preserved than previously anticipated. Perhaps the apparent absence of feathers in many specimens is due to their nonrecognition and subsequent destruction during fossil preparation. This potential for feather preservation in fluvial deposits, combined with the sheer abundance of non-avian dinosaurs found in such rocks, reveals great new possibilities for the discovery of feathered dinosaurs worldwide.

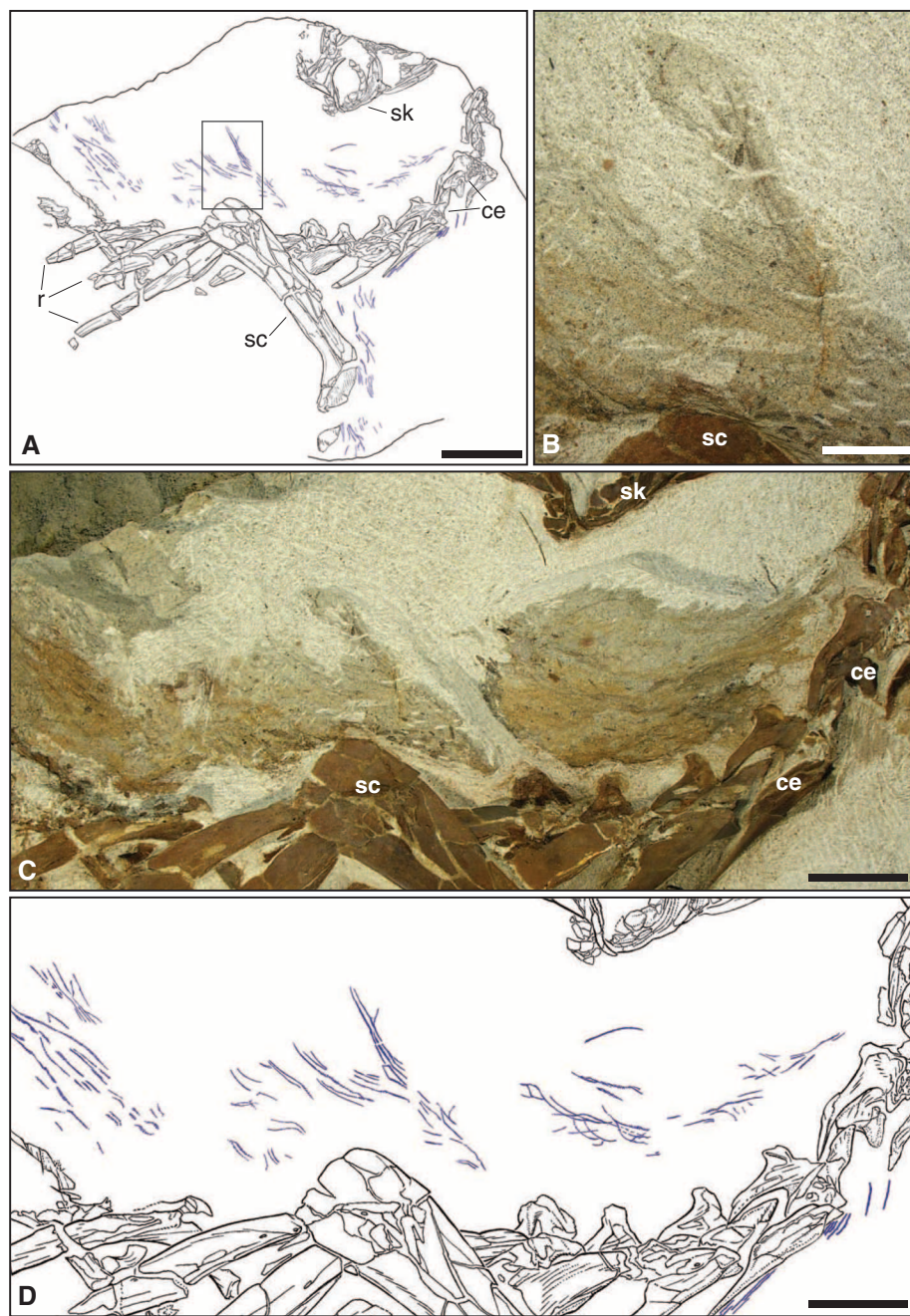
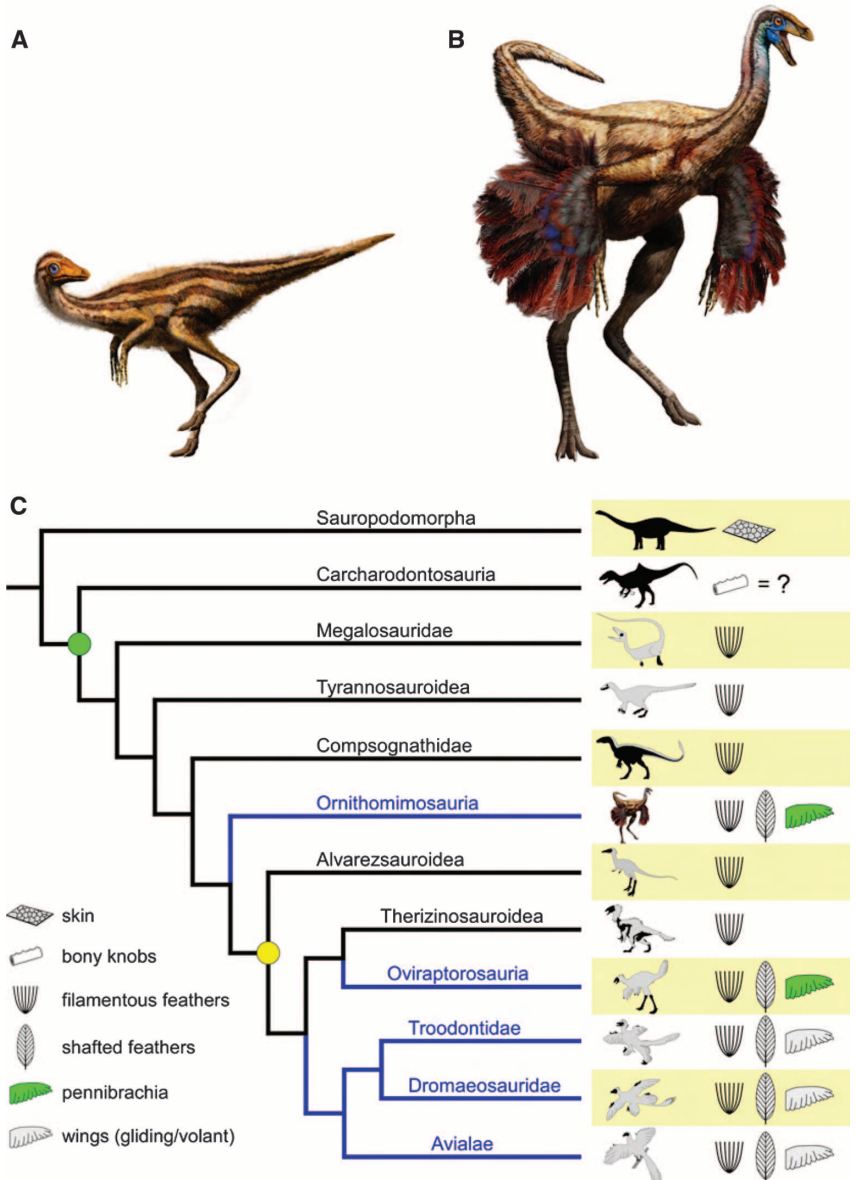


Fig. 2. Adult *Ornithomimus* (TMP 2008.70.1), preserving carbonized filamentous feathers. (A) Illustration of specimen showing the distribution and orientation of filamentous feathers (blue). Scale bar, 10 cm. (B) Close-up of curved filamentous feathers in inset from (A). Scale bar, 2 cm. (C) Photograph and (D) illustration of filamentous feathers along the dorsal side of the vertebral column. Scale bar, 5 cm. ce, cervical vertebrae; r, rib; sc, scapula; sk, skull.

Fig. 3. Adult *Ornithomimus* skeleton (TMP 1995.110.1), preserving evidence of shafted feathers. (A) Region of markings on the forelimb bones, delineated by a black rectangle. Scale bar, 50 cm. (B) Close-up of ulna (on left) and radius showing markings. Scale bar, 2 cm. (C) Schematic drawing of inset from (B), illustrating the shape, orientation, and distribution of markings on a portion of the ulna. U- and hook-shaped components are shown in blue. Scale bar, 1 cm.



Fig. 4. Ornithomimosaur plumage and its phylogenetic context. Artistic representations of (A) juvenile plumage and (B) adult plumage, both illustrated by Julius Csotonyi. (C) Phylogenetic distribution of major feather types and wings/pennibrachia in theropods. “Filamentous feathers” refer to all feathers that lack a rigid shaft [types 1, 2, and 3b of (11) and morphotypes 2 to 7 of (3)], whereas “shafted feathers” refer to all feathers that possess a rigid shaft [types 3a, 3a+b, 4, and 5 of (11) and morphotypes 8 and 9 of (3)]. Theropod phylogeny is from (35), and the reported occurrences of feathers are from (2, 36). The basalmost occurrence of winglike structures among Theropoda is in Ornithomimosauria. Forearm protuberances in a basal carcharodontosaur have been suggested to be associated with non-scale skin appendages (37) of unknown type. Green node, Theropoda. Yellow node, Maniraptora. Blue branches indicate clades that possess wings/pennibrachia. Gray wings denote clades in which at least one taxon used wings for aerial locomotion.



References and Notes

1. M. A. Norell, X. Xu, *Annu. Rev. Earth Planet. Sci.* **33**, 277 (2005).
2. X. Xu, Y. Guo, *Vertebrat Palasiatica* **47**, 311 (2009).
3. X. Xu, X. Zheng, H. You, *Nature* **464**, 1338 (2010).
4. Z. Zhou, P. M. Barrett, J. Hilton, *Nature* **421**, 807 (2003).
5. Z. Fucheng, Z. Zhonghe, G. Dyke, *Geol. J.* **41**, 395 (2006).
6. X. Xu *et al.*, *Nature* **484**, 92 (2012).
7. D. Hu, L. Hou, L. Zhang, X. Xu, *Nature* **461**, 640 (2009).
8. See the supplementary materials on Science Online.
9. Q. Ji, P. J. Currie, M. A. Norell, J. Shu-An, *Nature* **393**, 753 (1998).
10. P. J. Chen, Z. M. Dong, S. N. Zhen, *Nature* **391**, 147 (1998).
11. R. O. Prum, A. H. Brush, *Q. Rev. Biol.* **77**, 261 (2002).
12. R. O. Prum, *J. Exp. Zool.* **285**, 291 (1999).
13. M. H. Schweitzer *et al.*, *J. Exp. Zool.* **285**, 146 (1999).
14. X. Xu, Z. Tang, X. Wang, *Nature* **399**, 350 (1999).
15. C. Dal Sasso, M. Signore, *Nature* **392**, 383 (1998).
16. D. E. G. Briggs, P. R. Wilby, B. P. Pérez-Moreno, J. L. Sanz, M. Fregenal-Martínez, *J. Geol. Soc. London* **154**, 587 (1997).
17. A. W. A. Kellner, *Nature* **379**, 32 (1996).
18. P. G. Davis, D. E. G. Briggs, *Geology* **23**, 783 (1995).
19. A. W. A. Kellner, in *Mesozoic Birds above the Heads of Dinosaurs*, L. M. Chiappe, L. M. Witmer, Eds. (Univ. of California Press, Berkeley, CA, 2002), pp. 389–404.
20. A. M. Lucas, P. R. Stettenheim, *Avian Anatomy. Integument, Part I* (U.S. Government Printing Office, Washington, DC, 1972).
21. R. S. Wray, *Proc. Zool. Soc. London* **55**, 343 (1887).
22. C. Sullivan, D. W. E. Hone, X. Xu, F. Zhang, *Proc. Biol. Sci.* **277**, 2027 (2010).
23. W. J. Bock, *Syst. Zool.* **14**, 272 (1965).
24. X. Xu *et al.*, *Nature* **421**, 335 (2003).
25. D. W. Fowler, E. A. Freedman, J. B. Scannella, R. E. Kambic, *PLoS ONE* **6**, e28964 (2011).
26. J. H. Ostrom, *Q. Rev. Biol.* **49**, 27 (1974).
27. K. P. Dial, *Science* **299**, 402 (2003).
28. A. M. Heers, K. P. Dial, *Trends Ecol. Evol.* **27**, 296 (2012).
29. L. E. Zanno, P. J. Makovicky, *Proc. Natl. Acad. Sci. U.S.A.* **108**, 232 (2011).
30. J. E. Duerden, *Agric. J. Union S. Afr.* **1**, 29 (1911).
31. F. B. Gill, *Ornithology* (W.H. Freeman, New York, ed. 3, 2007).
32. P. Cho, R. Brown, M. Anderson, *Zoo Biol.* **3**, 133 (1984).
33. S. Davies, *Ratites and Tinamous* (Oxford Univ. Press, Oxford, 2002).
34. D. E. Fastovsky, in *The Age of Dinosaurs. Short Courses in Paleontology 2*, S. J. Culver, Ed. (Paleontological Society, Knoxville, TN, 1989), pp. 22–33.
35. A. H. Turner, D. Pol, J. A. Clarke, G. M. Erickson, M. A. Norell, *Science* **317**, 1378 (2007).
36. O. W. M. Rauhut, C. Foth, H. Tischlinger, M. A. Norell, *Proc. Natl. Acad. Sci. U.S.A.* **109**, 11746 (2012).
37. F. Ortega, F. Escaso, J. L. Sanz, *Nature* **467**, 203 (2010).

Acknowledgments: We thank P. Andrew (landowner), D. Brinkman (logistical support), J. Csotonyi (artwork), D. MacLeod (specimen preparation), M. Newbrey (discussions), D. Sloan (technical illustrations), and K. Womble (graphics). Research was funded by the Royal Tyrrell Museum of Palaeontology, a Natural Sciences and Engineering Research Council of Canada Discovery grant (D.K.Z.), the University of Calgary Start-up Fund (D.K.Z.), and an NSF Division of Earth Sciences grant (EAR 0959029) (G.M.E.). TMP 1995.110.1, TMP 2008.70.1, and TMP 2009.110.1 are permanently deposited at the Royal Tyrrell Museum, Drumheller, Alberta, Canada.

Supplementary Materials

www.sciencemag.org/cgi/content/full/338/6106/510/DC1

Supplementary Text

Figs. S1 to S6

Tables S1 and S2

References (38–60)

30 May 2012; accepted 30 August 2012

10.1126/science.1225376

Australopithecus afarensis Scapular Ontogeny, Function, and the Role of Climbing in Human Evolution

David J. Green^{1*} and Zeresenay Alemseged²

Scapular morphology is predictive of locomotor adaptations among primates, but this skeletal element is scarce in the hominin fossil record. Notably, both scapulae of the juvenile *Australopithecus afarensis* skeleton from Dikika, Ethiopia, have been recovered. These scapulae display several traits characteristic of suspensory apes, as do the few known fragmentary adult australopithecine representatives. Many of these traits change significantly throughout modern human ontogeny, but remain stable in apes. Thus, the similarity of juvenile and adult fossil morphologies implies that *A. afarensis* development was apelike. Additionally, changes in other scapular traits throughout African ape development are associated with shifts in locomotor behavior. This affirms the functional relevance of those characteristics, and their presence in australopithecine fossils supports the hypothesis that their locomotor repertoire included a substantial amount of climbing.

Scapular morphology corresponds closely with locomotor habits, often irrespective of phylogeny (1–7). However, our understanding of this important element in hominin evolution is limited by the paucity of scapular fossil remains. Upon its discovery, the right scapula associated with the juvenile *Australopithecus afarensis* skeleton from Dikika, Ethiopia (DIK-1-1, “Selam”) represented the most complete such fossil known for this well-documented early hominin species (8). Furthermore, comparison of this complete juvenile with adult australopithecine fossils promised to

shed light on *A. afarensis* growth and development (8, 9). Continued preparation has since freed both scapulae from the matrix encasing much of the axial skeleton (Fig. 1).

Before DIK-1-1’s discovery, the limited number of available fossil scapulae provided only tentative clues that the australopithecine shoulder was apelike (10). In addition, we lack a clear understanding of what the scapular morphology of the last common ancestor (LCA) of *Pan* and *Homo* looked like, making it difficult to determine whether australopithecines retained apelike features from the LCA or if these features evolved independently (11–14). Furthermore, limited information on the postcranial architecture, developmental pathways, and the manner in which behavioral variation contributes to morphological diversity among extant hominoids presents a challenge for reconstruct-

ing locomotor patterns in extinct taxa. Here, we describe further the DIK-1-1 scapulae and infer the locomotor behavior of *Australopithecus* through comparisons with other fossil hominins—including the new specimen from Woranso-Mille, Ethiopia (KSD-VP-1/1) (15)—and modern apes and humans (16). We track the ontogeny of scapular shape among extant hominoids to evaluate how juvenile scapular morphology compares with the adult form. We also evaluate functionally relevant characters throughout development to identify various genetic and epigenetic influences on hard-tissue morphology. These approaches consider how ontogenetic shifts in locomotor behavior (e.g., in *Pan* and *Gorilla*) influence scapular shape, providing context for evaluating the morphology of more fragmentary adult fossils and a more comprehensive view for inferring the locomotor implications of australopithecine shoulder anatomy.

The original analysis of the right DIK-1-1 scapula showed it to be most similar to that of juvenile *Gorilla* (8), but the two principal component axes describing its shape explained only ~7% of variance, drawing criticism (15). We performed two canonical variates analyses (CVAs) among juvenile and adult representatives of modern *Homo*, *Pan*, *Gorilla*, and *Pongo*, as well as DIK-1-1 and the immature *H. ergaster* (early *H. erectus*) scapula of the Turkana Boy (KNM-WT 15000) (17). In the first CVA, *Homo* and *Pongo* separated from *Pan* and *Gorilla* along the first root axis, which accounted for 70.3% of the variation; *Pongo* and *Pan* separated from *Homo* and *Gorilla*, respectively, along the second root axis (16.0%; Fig. 2A). The DIK-1-1 scapulae did not significantly differ from one another ($P = 0.81$) and were most similar to those of *Gorilla* juveniles (table S6; KNM-WT 15000 fell among the juvenile *Homo* data (Fig. 2A). The second CVA considered fewer variables to include the less complete KSD-VP-1/1,

¹Department of Anatomy, Midwestern University, Downers Grove, IL 60515, USA. ²Department of Anthropology, California Academy of Sciences, San Francisco, CA 94118, USA.

*To whom correspondence should be addressed. E-mail: dgreen1@midwestern.edu